SUPPLEMENTARY MATERIAL

HuD (ELAVL4) gain-of-function impairs neuromuscular junctions and induces apoptosis in familial and sporadic amyotrophic lateral sclerosis models

Beatrice Silvestri[1,2], Michela Mochi[1], Darilang Mawrie[3], Valeria de Turris[2], Alessio Colantoni[1,2], Beatrice Borhy[1], Maria Giovanna Garone[4], Christopher Patrick Zammerilla[3], Udai B. Pandey[3] and Alessandro Rosa[1,2,*]

1. Department of Biology and Biotechnologies “Charles Darwin”, Sapienza University of Rome, Rome, Italy.
2. Center for Life Nano- & Neuro-Science, Fondazione Istituto Italiano di Tecnologia (IIT), Rome, Italy.
3. Department of Pediatrics and Neurology, University of Pittsburgh Medical Center, PA, USA.
4. Department of Stem Cell Biology, Murdoch Children’s Research Institute, The Royal Children's Hospital, Parkville, Melbourne, Victoria, Australia.

* corresponding author: alessandro.rosa@uniroma1.it

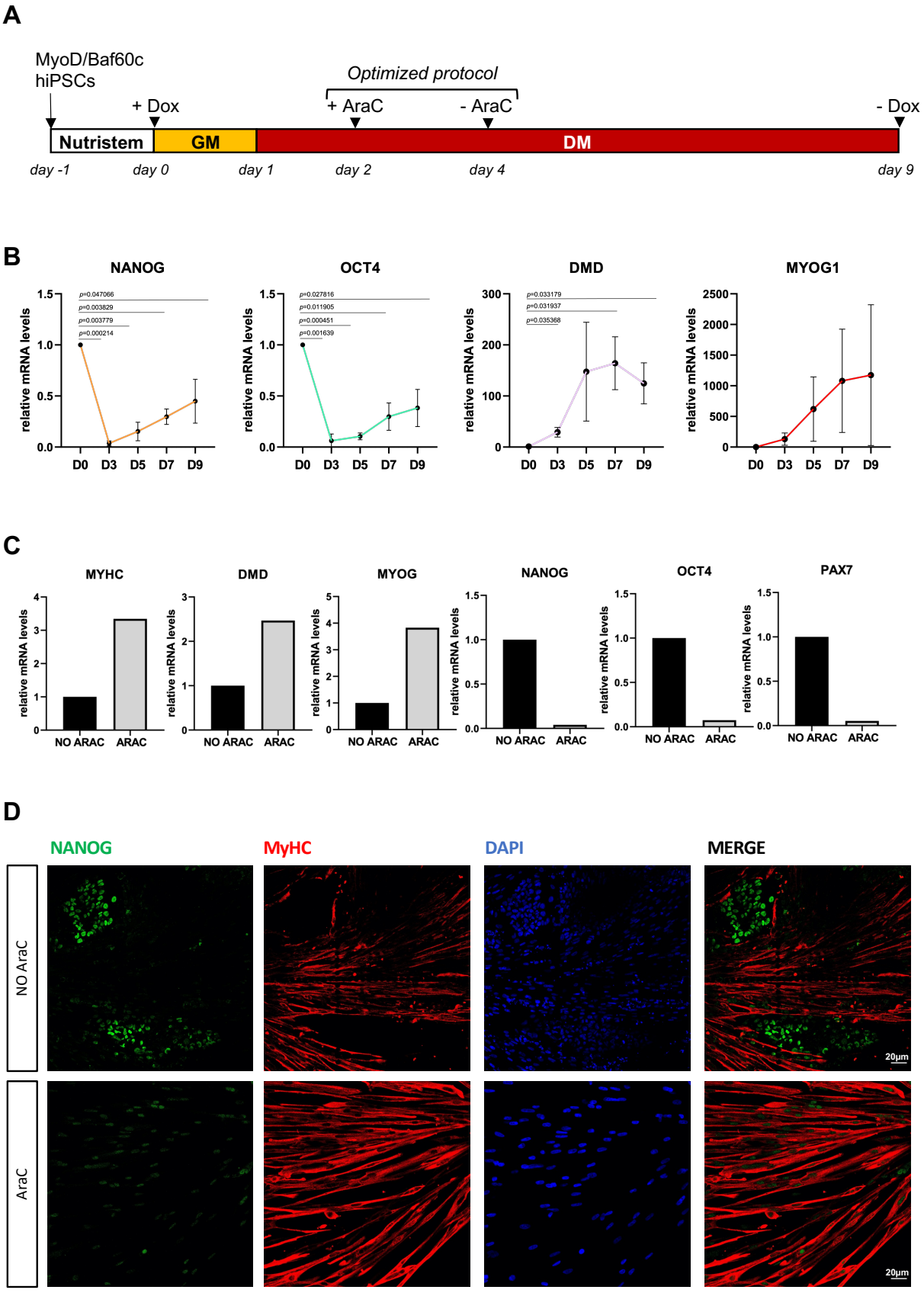
A
MyoD/Baf60c
hiPSCs
+ Dox
Optimized protocol
+ AraC
- AraC
- Dox
Nutristem
GM
DM
day -1
day 0
day 1
day 2
day 4
day 9
B
NANOG
OCT4
DMD
MYOG1
relative mRNA levels
D0 D3 D5 D7 D9
C
MYHC
DMD
MYOG
NANOG
OCT4
PAX7
NO ARAC
ARAC
D
NANOG
MyHC
DAPI
MERGE
NO AraC
AraC
20µm

Supplementary Figure S1. Optimization of the skeletal muscle differentiation protocol. Related to Figure 1.

(A) Schematic representation of the iPSC differentiation method to obtain SkMCs. (B) qRT-PCR expression analysis of pluripotency (*NANOG*, *OCT4*) and differentiation (*DMD*, *MYOG1*) markers, normalized on ATP5O expression, at the indicated time points (Day 0, 3, 5, 7, 9) from differentiation experiments performed without the use of cytosine arabinoside (AraC) at days 2 to 4 of the protocol, i.e. using the original method described in (Lenzi et al., 2016). Error bars indicate standard deviation (n=3 Student's t-test, paired, two tails). (C) Comparative qRT-PCR analysis of the expression of stemness/pluripotency (*PAX7*, *OCT4*, *NANOG*) and muscle (*DMD*, *MYOG1* and *MYHC*) markers at day 13 of differentiation (n=1), using the original (NO AraC) or optimized (AraC) protocol. ATP5O expression was used for normalization. (D) Immunofluorescence analysis of SkMCs as in (C). Nuclei were stained with DAPI (blue). Scale bar: 20μm.

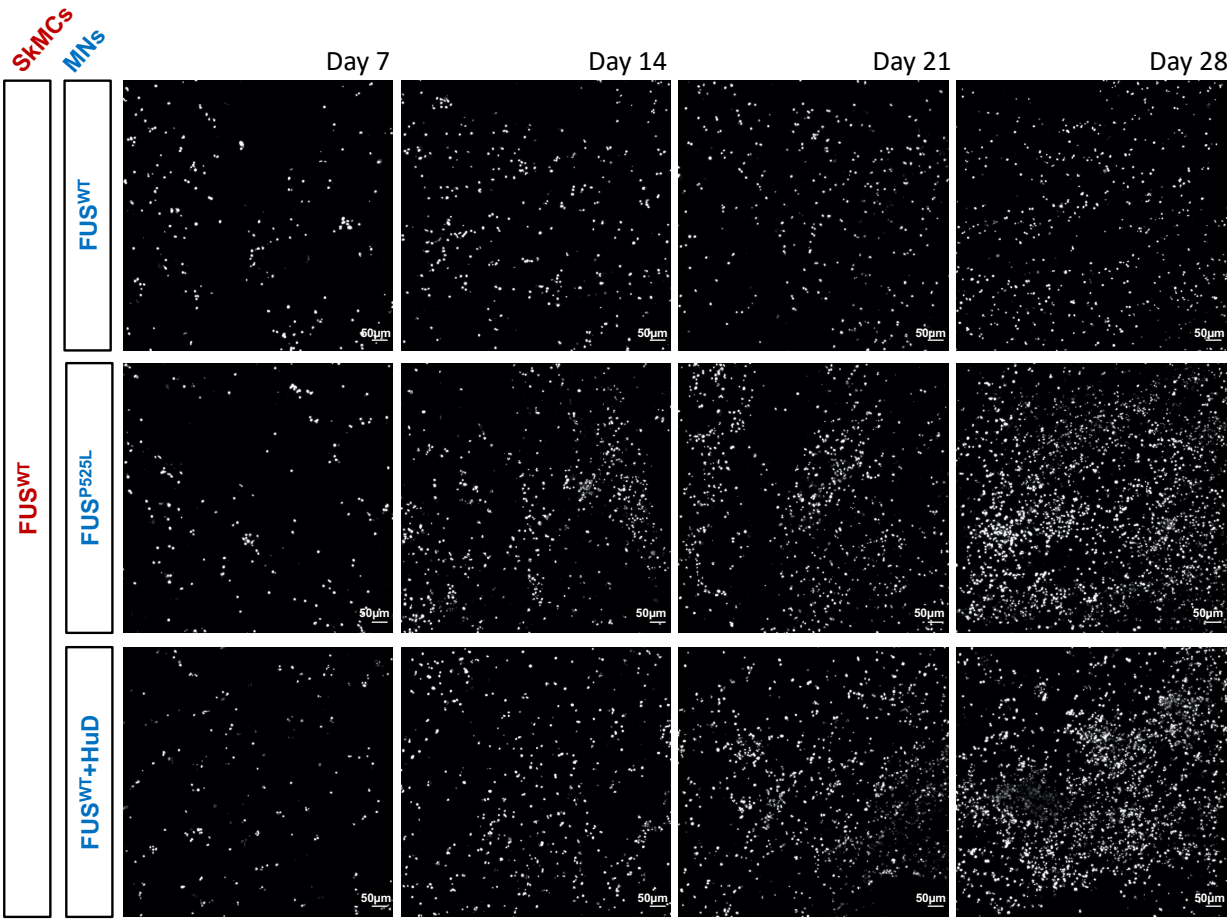

Supplementary Figure S2. Dead cell staining. Related to Figure 4.
Representative images of co-cultures stained with Ethidium Homodimer-1 (gray), used for quantification shown in Figure 4B. Scale bar: 50µm.

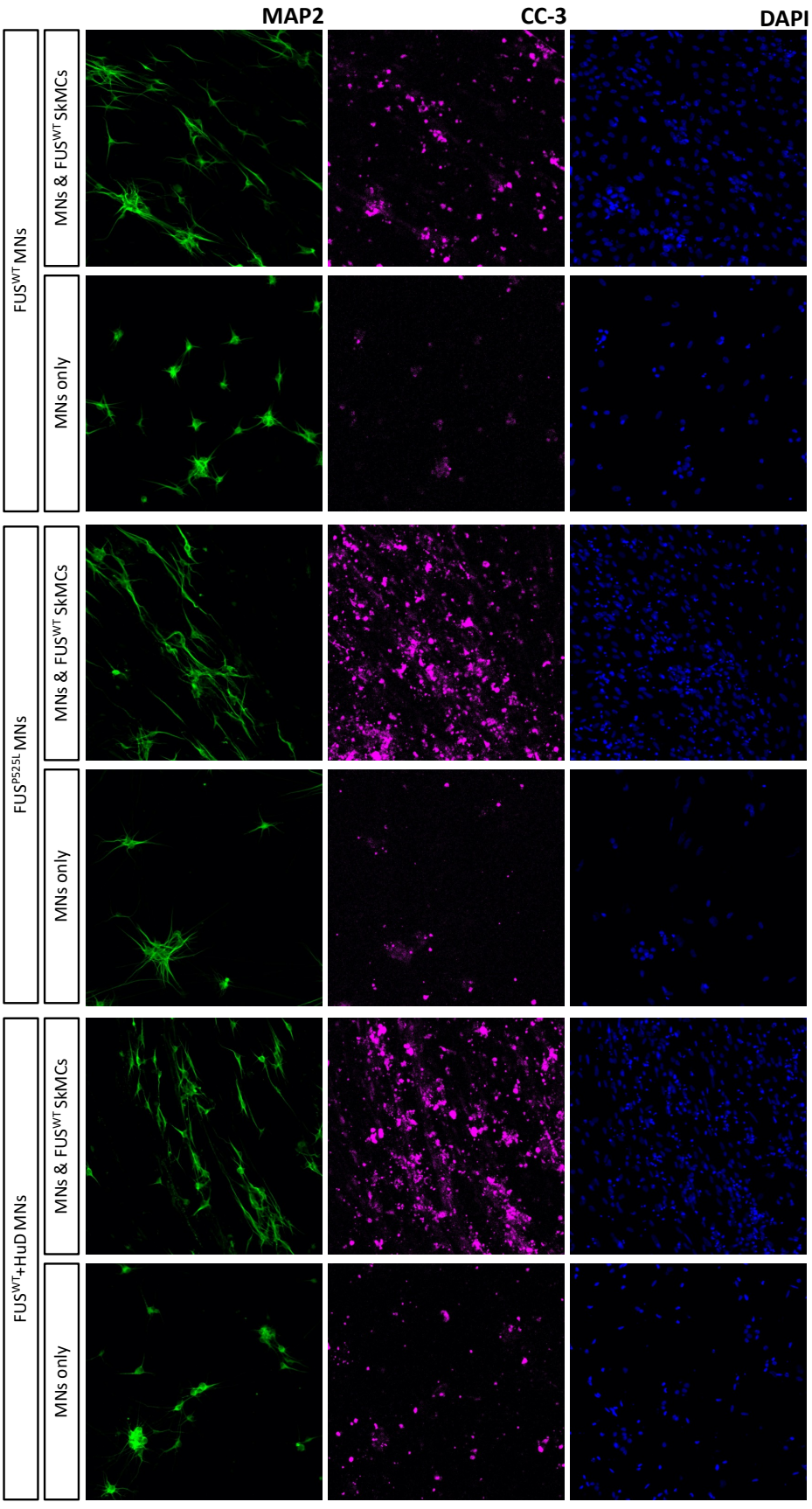

Supplementary Figure S3. Single panels of immunofluorescence staining. Related to Figure 4.

Single panels of immunofluorescence staining, shown in Figure 4C as merged images, of co-cultures or MN monocultures at day 14, using Cleaved Caspase-3 (CC-3) and MAP2 antibodies, and DAPI.

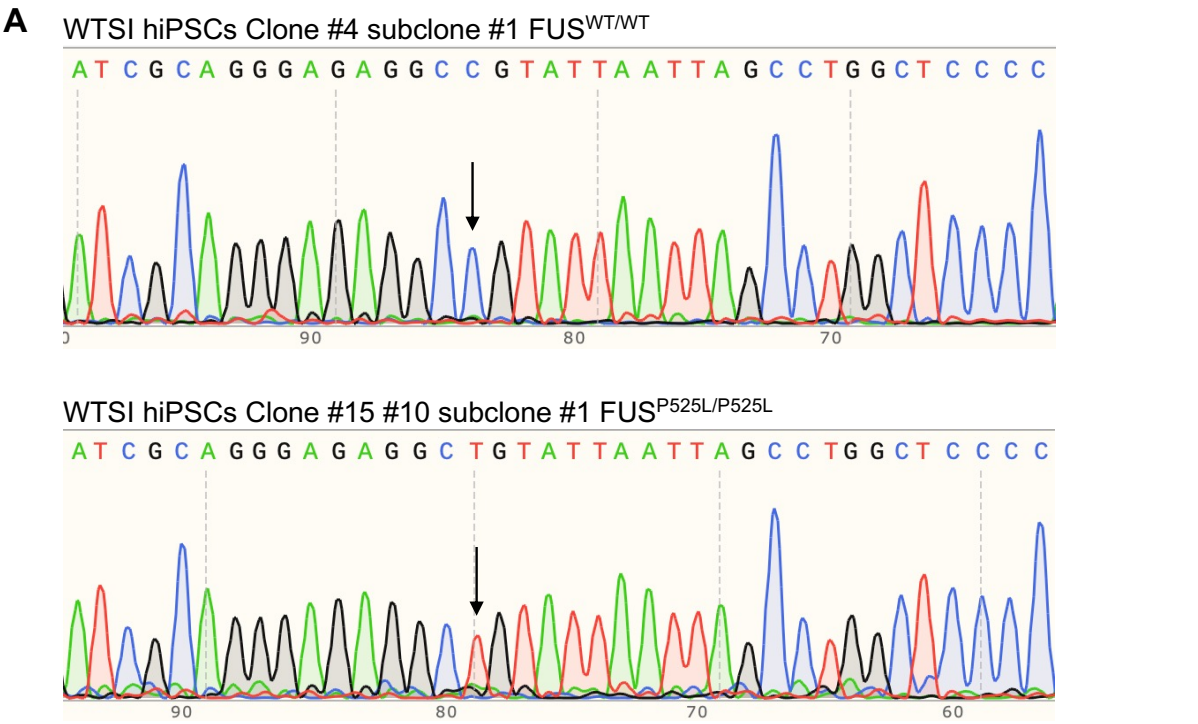

Supplementary Figure S4. Generation and characterization of the new FUS^{P525L} mutant line derived from WTSIi004-A iPSCs. Related to Figure 4.

(A) Sanger sequencing of a wild-type clone (top) and a FUS^{P525L} mutant (bottom) clone derived from the WTSIi004-A iPSC line (EBiSC) as previously described (Lenzi et al., 2015). These lines are named WTSI-FUS^{WT} and WTSI-FUS^{P525L} in the present paper. Arrows indicate the targeted nucleotide in codon 525: C, wild type; T, mutant. (B) Analysis of *HuD* mRNA levels in WTSI-FUS^{WT} and WTSI-FUS^{P525L} spinal MNs at day 12 of differentiation. TUBB3 has been used for normalization (n=1). (C) The graph reports quantitative analysis of the percentage of α-BTX positive fibers at day 14 of co-cultures made with FUS^{WT} SkMCs and WTSI-FUS^{WT}, WTSI-FUS^{P525L}, or WTSI-FUS^{WT}+HuD spinal MNs, as indicated. Error bars indicate standard deviation (n=3, Student's t-test; unpaired; two tails). (D) The graph reports quantitative analysis of the CC-3 fluorescence intensity at day 14 of co-cultures as in (C). Error bars indicate standard deviation (n=3, Student's t-test; unpaired; two tails).

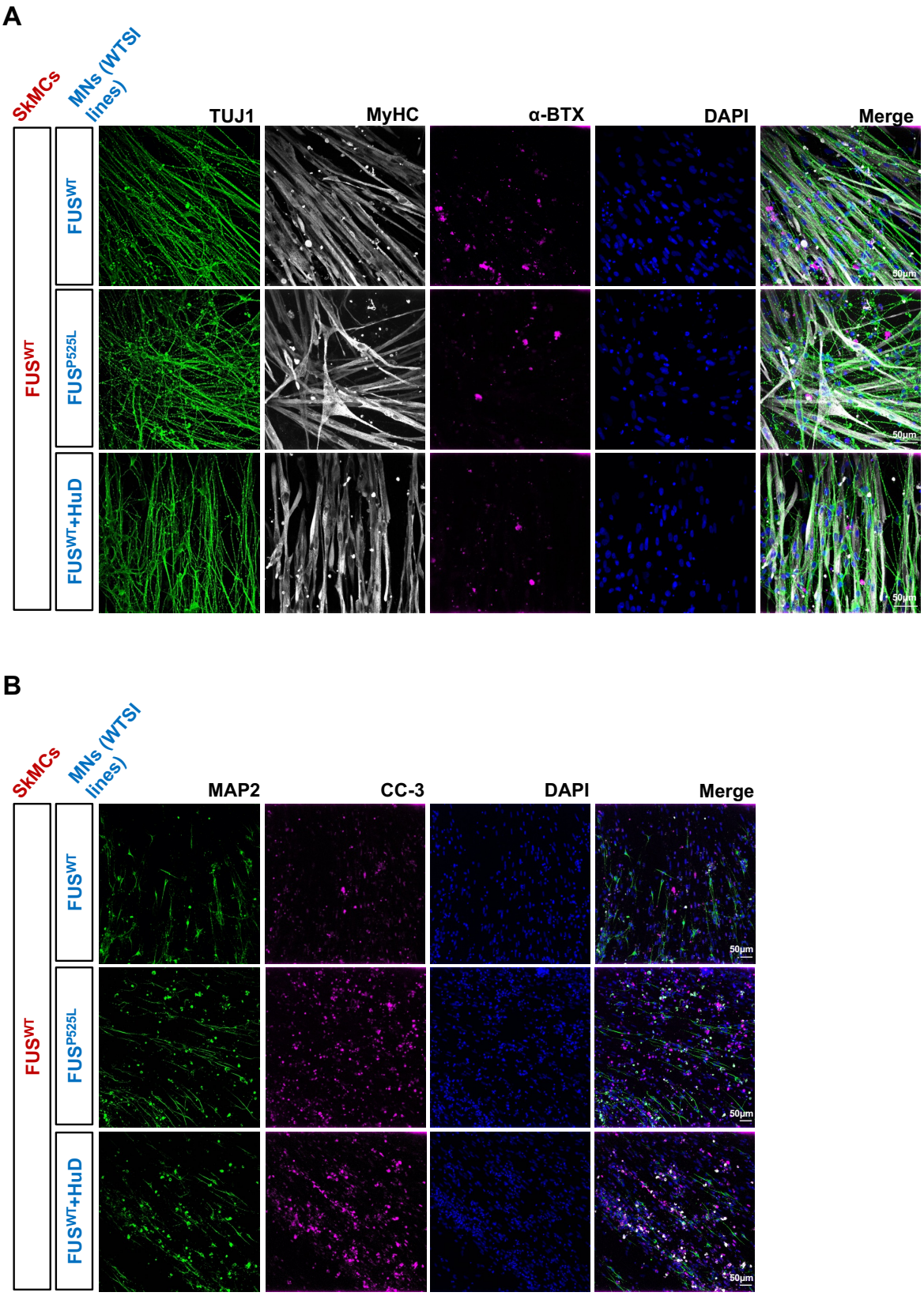

Supplementary Figure S5. Images used for quantification (WTSI co-cultures). Related to Figure 4.

(A-B) Images used for quantification analyses of Supplementary Figure S4C (panel A) and Supplementary Figure S4D (panel B). Scale bar: 50µm.

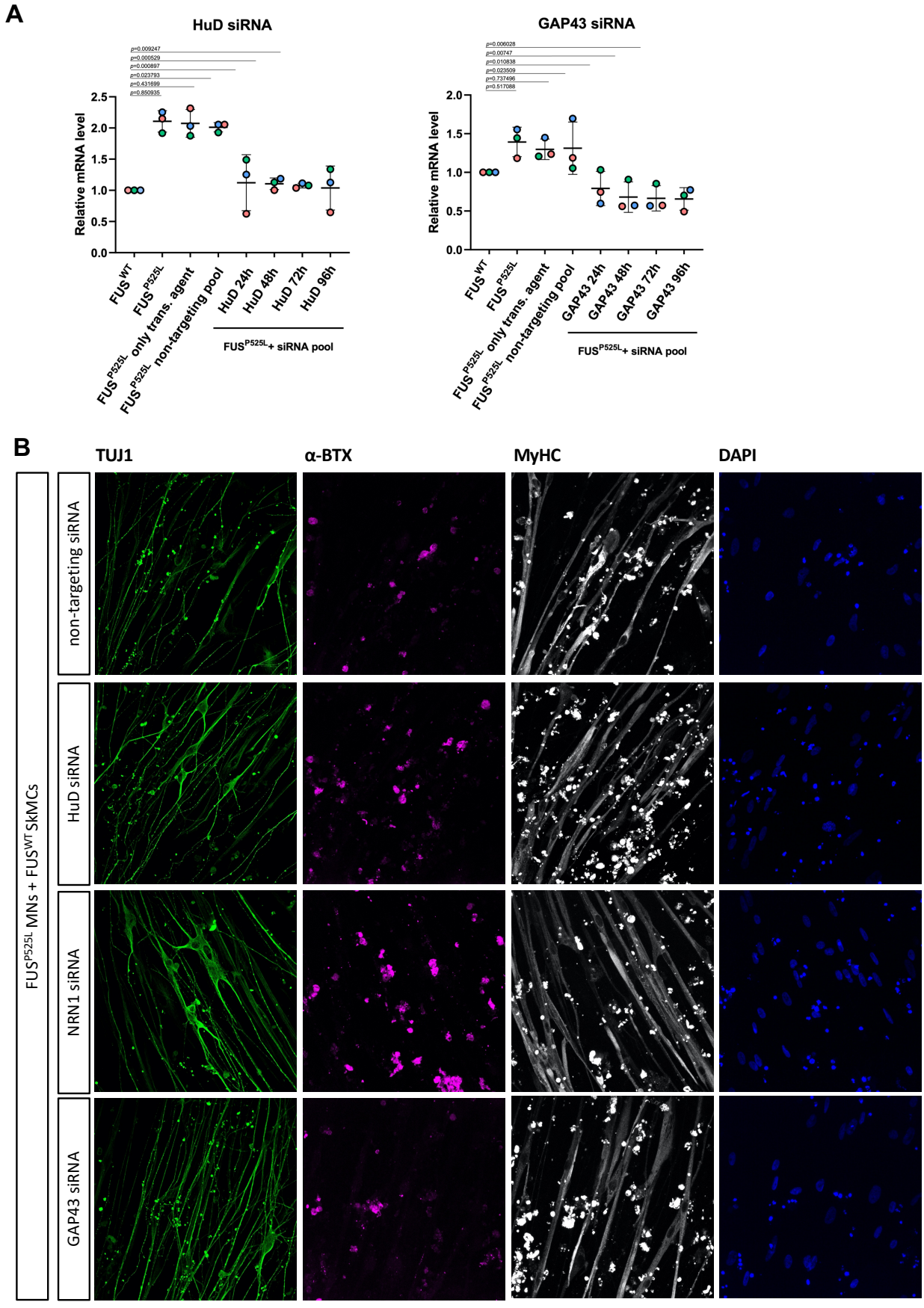
A
HuD siRNA
GAP43 siRNA
Relative mRNA level
FUS WT
FUS P525L
FUS P525L only trans. agent
FUS P525L non-targeting pool
HuD 24h
HuD 48h
HuD 72h
HuD 96h
GAP43 24h
GAP43 48h
GAP43 72h
GAP43 96h
FUS P525L+ siRNA pool
B
TUJ1
α-BTX
MyHC
DAPI
FUS P525L MNs + FUS WT SkMCs
non-targeting siRNA
HuD siRNA
NRN1 siRNA
GAP43 siRNA

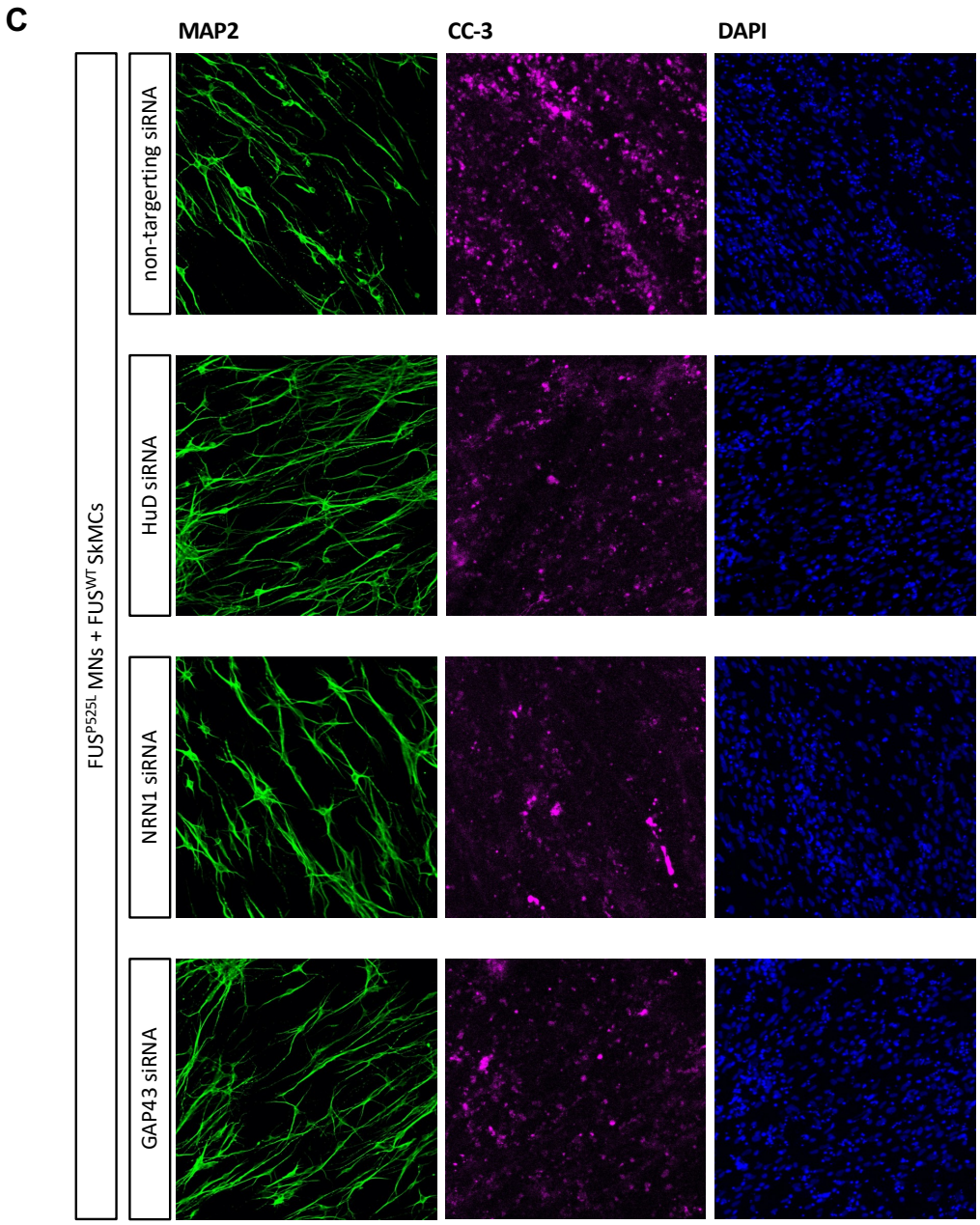

Supplementary Figure S6. Knockdown by RNAi in FUS^{P525L} MNs and co-cultures. Related to Figure 5.

(A) Analysis of *HuD* (left) and *GAP43* (right) mRNA levels in untransfected FUS^{WT} and FUS^{P525L} spinal MNs and FUS^{P525L} spinal MNs transfected with non-targeting control siRNA or siRNAs targeting *HuD* or *GAP43*. *ATP5O* has been used for normalization. Values indicated in the graphs are relative to untransfected FUS^{WT} samples. The graphs show the average and standard deviation from a biological triplicate (Student's t-test; unpaired; two tails). The same analysis for validating siRNAs targeting NRN1, used in the present work, had been previously reported (Garone et al., 2021). (B,C) Single panels of the immunofluorescence staining, shown in Figure 5A,B as merged images, of co-cultures made with FUS^{WT} SkMCs and FUS^{P525L} MNs.

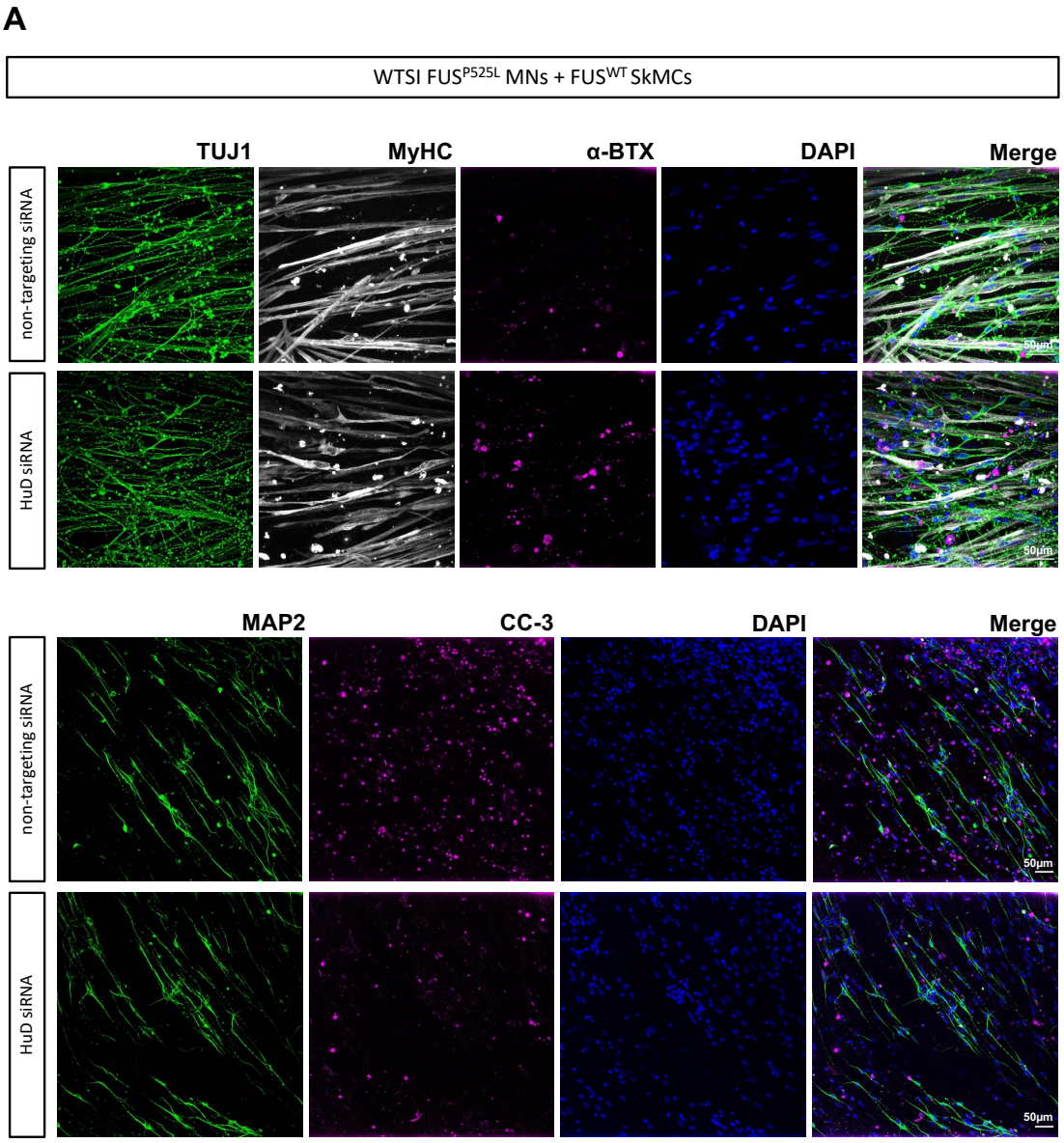

Supplementary Figure S7. HuD knockdown in co-cultures containing WTSI-FUS^{P525L} MNs. Related to Figure 5.

(A) Representative images of day 14 co-cultures obtained with FUS^{WT} SkMCs and WTSI-FUS^{P525L} MNs transfected with non-targeting control or HuD siRNAs and stained with the indicated antibodies.

Scale bar: 50μm. (B) The graphs report quantitative analysis of the percentage of α-BTX positive fibers (left) and CC-3 fluorescence intensity (right), at day 14 of co-culture as in (A). The graphs show the average and standard deviation from a biological triplicate (Student’s t-test; unpaired; two tails).

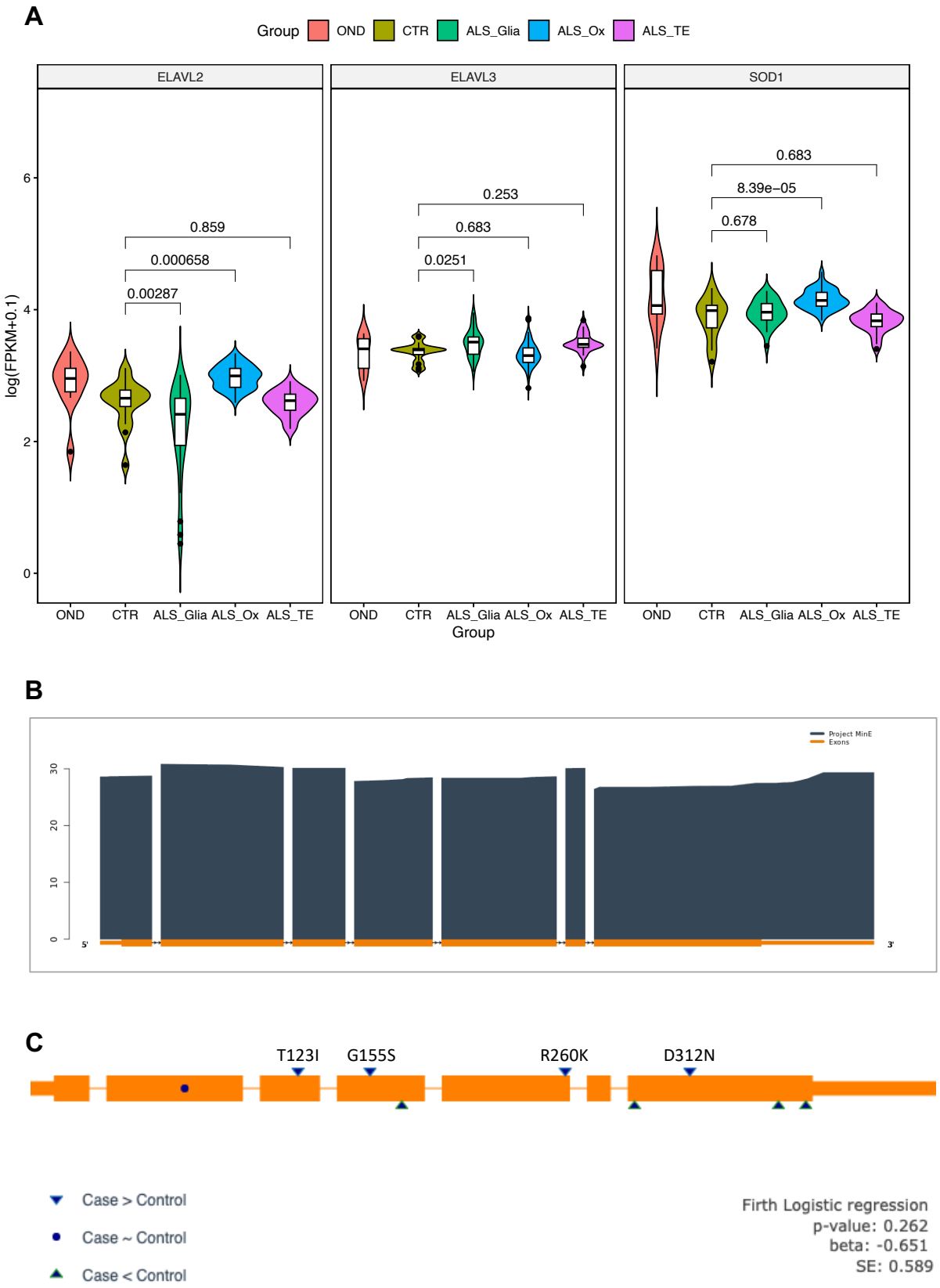

Supplementary Figure S8. Analysis of nELAVLs and SOD1 expression in sporadic ALS patients and *HuD* variants. Related to Figure 7.

(A) Violin plots showing the expression levels, reported as log-transformed FPKM values, of *ELAVL2* (*HuB*), *ELAVL3* (*HuC*) and *SOD1* in post-mortem sporadic ALS patients' cortex samples from (Tam

et al., 2019). OND: other neurodegenerative diseases; CTR: healthy individuals; ALS_Glia: sporadic ALS patients with a signature of glial activation; ALS_Ox: sporadic ALS patients with a signature of oxidative and proteotoxic stress; ALS_TE: sporadic ALS patients with a signature of high retrotransposon expression. The adjusted *p*-values obtained from differential expression analyses are shown. (B-C) Snapshots of the Project MinE data browser (http://databrowser.projectmine.com): coverage of the *HuD* gene (B) and exons (orange blocks) with the variants (triangles) that are reported in the current dataset (C). Variants that have been found with a higher frequency in ALS cases than controls are indicated.

Supplementary Table S1. List of primers used in this study.

Name	Sequence or assay
NANOG FW	CCAAATTCTCCTGCACGTGAC
NANOG RV	CACGTGGTTTCCAAACAAGAAA
ATP5O FW	ACTCGGGTTTGACCTACAGC
ATP5O RV	GGTACTGAAGCATCGCACCT
HuD FW	CAACCCCAGCCAGAAGTCCA
HuD RV	AGCCTGAACCTCTGAGCCTG
NRN1 FW	GGCTTTTCGGACTGTTTGCTCA
NRN1 RV	ATCCTCCCAGTATGTGCACACG
GAP43 FW	GAGGAGCCTAAACAAGCCGATG
GAP43 RV	GGGCACTTTCCTTAGGTTTGGT
MYH1	Hs_MYH1_2_SG QuantiTect Primer Assay, QT01671005
MYOG	Hs_MYOG1_SG QuantiTect Primer Assay, QT00001722
DMD	Hs_DMD_1_SG QuantiTect Primer Assay, QT00085778
OCT4 FW	ATGCATTCAAACTGAGGTGCCTGC
OCT4 RV	AACTTCACCTTCCCTCCAACCAGT
PAX7 FW	CAGAGGACCAAGCTGACAGA
PAX7 RV	CTGGCAGAAGGTGGTTGAAC
SOD1 FW	TGAAGGTGTGGGGAAGCATT
SOD1 RV	TCTCTTCATCCTTTGGCCCA
TUBB3 FW	CCCGGAACCATGGACAGTGT
TUBB3 RV	TGACCCTTGGCCCAGTTGTT